Aus dem Institut Berlin-Brandenburg Center for Regenerative Therapies (BCRT)
der Medizinischen Fakultät Charité – Universitätsmedizin Berlin

DISSERTATION

High-frequency ultrasound backscatter analysis of hyaline cartilage

zur Erlangung des akademischen Grades
Doctor of Philosophy (PhD)

vorgelegt der Medizinischen Fakultät
Charité – Universitätsmedizin Berlin

von

Nils Stefan Männicke

aus Leipzig

Datum der Promotion: 16.06.2018

Contents

1 Introduction **3**

2 Materials and Methods **10**

2.1 Samples 10

2.2 Ultrasound measurements 10

2.3 Structural parameters 11

2.4 Ultrasound data analysis 11

2.5 Statistics 12

3 Results **13**

4 Discussion **15**

5 References **18**

6 Eidesstattliche Versicherung **21**

7 Anteilserklärung **21**

8 Publikationen **23**

8.1 3-D High-Frequency Ultrasound Backscatter Analysis of Human Articular Cartilage 23

8.2 3-D Articular Cartilage Degeneration Classification by means of High-Frequency Ultrasound 37

8.3 Species-Independent Modeling of High-Frequency Ultrasound Backscatter in Hyaline Cartilage 43

9 Lebenslauf **53**

10 Publikationsliste **54**

11 Danksagung **57**

Abstract

High-frequency ultrasound is a promising method to characterize osteoarthritic changes of cartilage tissue *in vivo*. Numerous studies have investigated the cartilage surface reflection and successfully related derived ultrasound surface parameters to the degeneration stage of cartilage. Only a few studies evaluated acoustic backscatter originating from the cartilage matrix and so far only integrated spectral amplitudes of the received signals have been considered, particularly the apparent integrated backscatter (AIB). However, information contained in the ultrasound frequency domain could potentially exhibit higher sensitivities towards degenerative changes at a cellular level and therefore provide additional information that may enable a better discrimination between degeneration stages.

The aims of this work were to introduce parameters that relate to the frequency dependence of ultrasound backscatter and envelope statistics, to study their diagnostic value in comparison with the well-established AIB, to attempt to classify different degeneration stages using combinations of ultrasound parameters and finally to study the contributions of collagen, proteoglycan and chondrocytes to ultrasound backscatter amplitude.

Results showed that the introduced apparent frequency dependence of backscatter (AFB) was sensitive to degenerative changes, particularly the earliest signs of degeneration, whereas the conventionally used AIB exhibited relatively low sensitivities. Furthermore, it was demonstrated that in a classification-based approach, combinations of ultrasound parameters can be used to discriminate between different, particularly very early, degeneration stages. Here, backscatter frequency dependence and backscatter amplitude appeared as good predictors for the discrimination of early and advanced degeneration stages, respectively. Finally, it was shown that more than 50% of the backscatter amplitude can be attributed to natural variations of cell number density and collagen concentration.

This work demonstrated for the first time that envelope statistics and depth-dependent spectral slope parameters are highly sensitive to the early stages of extracellular cartilage matrix degeneration and outperform conventionally used amplitude-based parameters. Moreover, these parameters provide beneficial additional information in a classification approach to discriminate between different degeneration stages. The identification of collagen and chondrocytes as major scattering sources at higher ultrasound frequencies suggests that the observed variations relate to degenerative changes of chondrocytes and the collagen network. An application of these parameters and particularly the use of parameter combinations to intra-articular ultrasound arthroscopies appears feasible at present and likely improves the diagnostic potential of these examinations.

Abstract

Hochfrequenter Ultraschall ist eine vielversprechende Methode um osteoarthritische Veränderungen von Gelenkknorpel *in vivo* zu erfassen. Die am häufigsten verwendeten Ultraschallparameter basieren auf der Verarbeitung von Ultraschallreflexionen an der Knorpeloberfläche und eine Vielzahl von Studien konnten Veränderungen dieser Parameter in Bezug zu osteoarthritischen Veränderungen setzen. Nur wenige Studien haben bisher die Ultraschallrückstreuung von der extrazellulären Knorpelmatrix untersucht und dabei wurden lediglich Parameter verwendet die einen Mittelwert des Frequenzbereichs darstellen, *i.e.* der apparent integrated backscatter (AIB). Die damit verlorengegangene frequenzabhängige Information könnte jedoch eine hohe Sensitivität auf degenerative zelluläre Veränderungen aufweisen und damit eine bessere Unterscheidung zwischen Degenerationsstadien ermöglichen.

Die Ziele dieser Arbeit waren die Einführung von Parametern die die frequenzabhängige Information adäquat abbilden sowie statistische Parameter der Einhüllenden, die vergleichende Untersuchung dieser Parameter hinsichtlich ihrer Sensitivität auf die zugrundeliegende Knorpelmatrixdegeneration, eine Klassifizierung zwischen verschiedenen Degenerationsstadien unter Verwendung mehrerer Ultraschallparameter, sowie die Untersuchung des Einflusses der Knorpelmatrixkomponenten Proteoglykangehalt, Kollagengehalt sowie Zelldichte auf die Ultraschallrückstreuamplitude.

Die Ergebnisse haben gezeigt, dass die Frequenzabhängigkeit des Amplitudenspektrums (apparent frequency dependence of backscatter, AFB) im Unterschied zum konventionellen AIB eine hohe Sensitivität auf degenerative Veränderungen, insbesondere sehr frühe Degenerationsstadien, aufzeigt. Weiterhin konnte gezeigt werden, dass eine Klassifikation zwischen unterschiedlichen, insbesondere sehr frühen, Degenerationsstadien mittels mehrerer Ultraschallparameter möglich ist. Die Verwendung von AFB und AIB war dabei hilfreich zur Unterscheidung früher bzw. fortgeschrittener Degenerationsstadien. Schlussendlich konnte gezeigt werden, dass mehr als 50% der Ultraschallrückstreuamplitude der natürlichen Variabilität von Kollagenhgehalt und Zelldichte zugeordnet werden kann.

Diese Arbeit konnte erstmals darlegen, dass frequenzabhängige Ultraschallparameter sowie statistische Parameter der Einhüllenden eine hohe Sensitivität auf frühe degenerative Veränderungen der Knorpelmatrix aufweisen und den konventionellen Parameter AIB deutlich übertreffen. Des Weiteren konnte die Klassifikation verschiedener Knorpeldegenerationsstadien durch Einbeziehung dieser Parameter verbessert werden. Die Identifikation von Chondrocyten und Kollagen als wichtige Rückstreuquelle hochfrequentem Ultraschalls deutet darauf hin, dass die beobachteten Veränderungen des AFB Degenerationen von Chondrocyten und des Kollagennetzwerks zugeordnet werden könnten. Eine Anwendung dieser Parameter für intra-artikuläre Ultraschallarthroskopien ist denkbar und könnte deren diagnostisches Potential deutlich erhöhen.

1 Introduction

Osteoarthritis (OA) is a common chronic disease that involves the progressive degeneration of hyaline cartilage within synovial joints and can affect any joint, most commonly the knee or hip joint and those of the hand. Common symptoms are joint pain and stiffness as well as reduced function and participation restriction, resulting in a severe loss of patient life quality. OA is age-related, with symptoms often appearing not before middle age. The prevalence is high: 24% and 11% in the general adult population show symptoms of OA of knee and hip joints, respectively [1]. In elderly people, OA is considered the most common cause of disability [2].

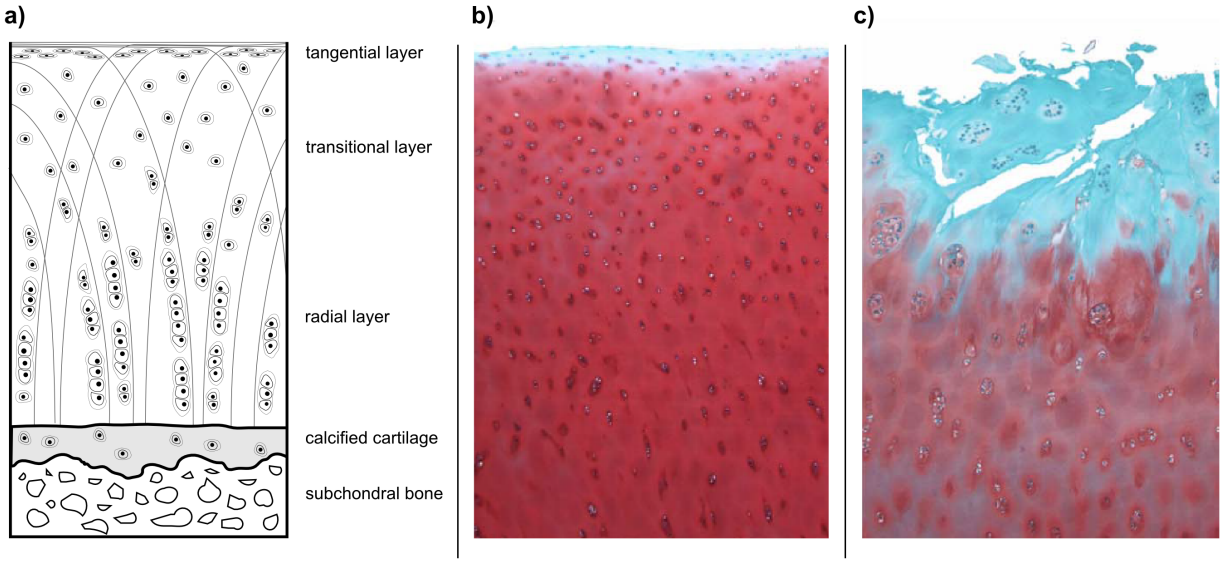

Figure 1: a): Layered structure of healthy articular cartilage. The superficial zone is characterized by a large number of small disk-shaped chondrocytes. Fewer and more isotropic chondrocytes can be observed in the transitional zone. In the radial zone, chondrons contain multiple chondrocytes. Cell density is lowest and the cell size is large. Note the arch-like structure of collagen, with the fiber orientation parallel to the surface in the superficial zone and perpendicular to the surface in the radial zone [3]. b): Hemotoxylin and eosin (H&E) stained histological cross-section of an intact cartilage sample (OARSI grade 0). c): H&E stained cross-section of a cartilage samples with moderate signs of degeneration (OARSI grade 3). Reprinted from [3, 4] with permission from Elsevier.

The structure of healthy hyaline cartilage is characterized by a distinct zonal organization with different collagen-orientations and cellular properties (Fig. 1). The earliest cartilage degeneration stages at the tissue level are cartilage tissue swelling and softening due to a loss of extracellular macromolecules, which results in a reduced capacity of the cartilage tissue to bind or release water. Subsequently, the superficial collagen becomes more prone to mechanical injury, resulting in a fibrillation and roughening of the superficial cartilage zones. Later stages are characterized by a disruption of the collagen network, Pannae (cracks), complete loss of biomechanical competence and ultimately, loss of cartilage tissue. Cellular

changes are manifested as diffuse hypercellularity, cell cloning and cell loss from earlier to later stage degenerations. All these changes can be verified histologically and various histopathological scoring systems exist, *e.g.* the Mankin score (Table 1) [5] or the more recent OARSI grading system [4].

The clinical diagnosis of OA is often based on radiographic images (X-ray). Radiography can assess bony features associated with OA, such as the presence of osteophytes, which is the most important criterion for radiographical OA diagnosis [6]. Narrowing of the joint space width as a result of a decrease in cartilage thickness is an indicator for disease progression. Moreover, subchondral bone sclerosis and potential bone deformities are indicators for later stage degenerations. The major drawback of radiographic imaging is its insensitivity to all non-mineralized tissue if no contrast agents are used, as is the case in a CT arthrography, for example. This implies that cartilage tissue thickness and meniscal integrity are assessable only indirectly through the joint spacing.

Table 1: Histological-histochemical grading (Mankin et al.)[5]. The sum of the four scores is typically referred to as Mankin score.

	Grade		Grade
I. Structure		**III. Safranin-O staining**	
a. Normal	0	a. Normal	0
b. Surface irregularities	1	b. Slight reduction	1
c. Pannus and surface irregularities	2	c. Moderate reduction	2
d. Clefts to transitional zone	3	d. Severe reduction	3
e. Clefts to radial zone	4	e. No dye noted	4
f. Clefts to calcified zone	5		
g. Complete disorganization	6		
II. Cells		**IV. Tidemark integrity**	
a. Normal	0	a. Intact	0
b. Diffuse hypercellularity	1	b. Crossed by blood vessels	1
c. Cloning	2		
d. Hypocellularity	3		

For this reason, magnetic resonance imaging (MRI) is becoming the most widely used modality for the assessment of joint structures in research [6, 7] as it enables an evaluation of OA as a whole organ disease. Several semi-quantitative MRI scoring systems for knee OA exist (*e.g.* WORMS, BLOKS, MOAKS, KOSS) [6], that assess degenerative morphologic changes of bone marrow, subchondral bone, cartilage, menisci, synovitis, and ligaments independently and are therefore able to evaluate the degenerative state in a more sophisticated and detailed manner compared to radiography. In addition to morphological MRI, compositional changes of cartilage and menisci extracellular matrix can be analyzed using well-established, advanced MR imaging techniques such as the T2-mapping and delayed gadolinium-enhanced MR imaging of cartilage (dGEMRIC). T2-mapping can quantitatively

determine the collagen concentration and orientation due to its sensitivity to the interaction of water with macromolecules [8]. dGEMRIC has been shown to be an indirect measure of glucosaminoglycans, the water-binding macromolecules of the cartilage extracellular matrix. The anionic gadolinium particles are able to diffuse into the cartilage matrix if the glucosaminoglycans are absent and the local anionic potential of the extracellular matrix is low. Hence, the detection of locally high concentrations of gadolinium is typically associated with a higher cartilage degeneration [8].

Arthroscopy is a minimally invasive surgical procedure in which a small fiberoptic endoscope is inserted into the joint that enables a reliable assessment of cartilage tissue and immediate surgical intervention. Treatments vary from washing out debris and crystals to prevent inflammation, debridement of torn menisci, smoothening the cartilage surface and removal of osteophytes that block the full extension of the joint [9]. In addition to optical images of the cartilage surface, the biomechanical competence of the tissue can be assessed by arthroscopic indentation devices, *e.g.* as proposed by Kiviranta et al. [10]. Moreover, Viren at al. [11] proposed the application of intravascular ultrasound (IVUS) devices during arthroscopy, *i.e.* intra-articular ultrasound (IAUS) which has been part of extensive research in the past years and recently shown to be feasible for *in vivo* applications [12] (Fig. 2). The major advantage of IAUS besides providing qualitative information such as imaging of lesions within the cartilage matrix, is the access it allows to a large number of quantitative ultrasound parameters that relate to the degenerative state of cartilage [13].

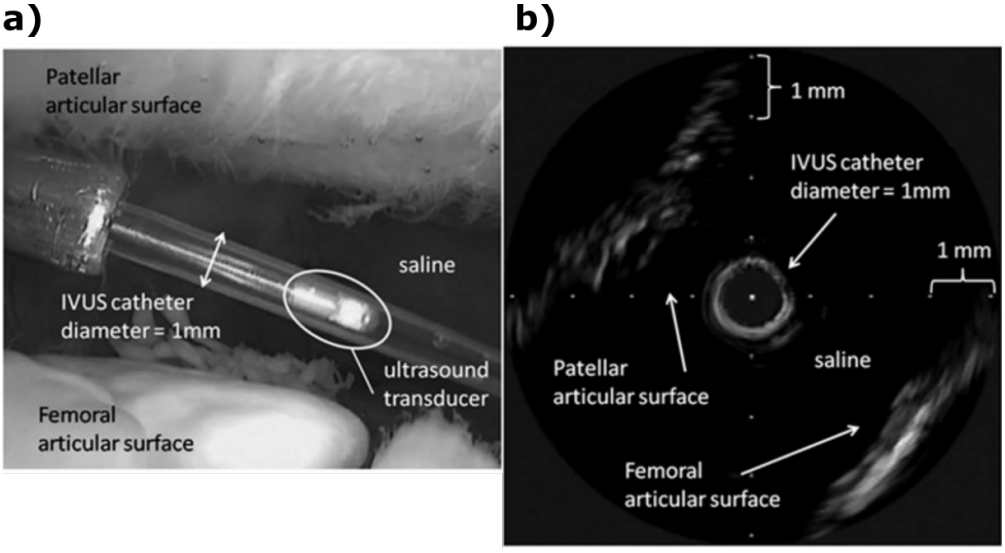

Figure 2: Images of arthroscopic video (a) and intra-articular ultrasound (b) during an *in vivo* application of IAUS. Patellar and femoral articular surfaces are visible. The femoral surface appears more fibrillated. Reprinted from [13] with permission from Sage.

Ultrasound is a mechanical wave that is transmitted through a medium by local displacements of particles of the medium, thereby causing temporal and spatial changes of medium density. Longitudinal wave propagation is the simplest form of wave propagation and is

valid for isotropic liquids, gases, and biological soft tissue. The longitudinal wave propagation speed c, *i.e.* speed of sound, is dependent on the compressibility of the medium. Other wave propagations, such as shear waves or Rayleigh waves, are apparent in solid materials and solid boundary surfaces, respectively. The wave propagation speed c is medium-specific and dependent on the medium compressibility and mass density. The ultrasound frequency f determines the number of oscillations per time unit and is inversely proportional to the wavelength λ:

$$f = \frac{c}{\lambda} \tag{1}$$

The axial resolution d_a, *i.e.* the resolution in direction of the beam propagation, of an ultrasound imaging system is dependent on the spatial pulse length τ:

$$d_a = \frac{c \cdot \tau}{2} = \frac{c \cdot \lambda \cdot j}{2} \tag{2}$$

,with j being the number of wavelengths contained in the emitted pulse, determined by the excitation duration of the ultrasound transducer. This means that axial resolution is directly correlated with the ultrasound frequency. The maximum lateral resolution is more complex, due to its dependence on the geometrical properties of the transducer, *e.g.* curvature and diameter of the aperture. However, the maximum possible lateral resolution is limited by the chosen ultrasound frequency.

Several main interactions occur between ultrasound waves and the medium as well as therein contained structures: Specular reflection, absorption, attenuation and scattering. Specular reflections occur at medium boundaries or structural boundaries with a dimension much larger than the wavelength. The amount of reflected energy is defined by the acoustic impedance difference between the two media. The remaining energy is transmitted. Absorption is the conversion of ultrasound energy into other forms of energy, *e.g.* thermal energy. Attenuation accounts for both absorption and scattering-processes. Attenuation coefficients are frequency-dependent and often expressed as:

$$\alpha = \alpha_0 \cdot f^n \tag{3}$$

,with both parameters α_0 and n as medium-specific parameters. For most biological tissues, n is larger than 1, which means that attenuation is increasing exponentially with increasing frequency.

Ultrasound scattering arises mostly from sub-wavelength structures. In contrast to specular reflections, the spectrum of scattered waves is usually not equivalent to that of incident waves and is direction dependent. As the name suggests, backscatter refers to scattering in the direction of the incident wave source and is most common in ultrasound measurements. Scattering intensity is highly dependent on the product of scatterer dimension a and

ultrasound wave number k, *i.e.* the ka-value:

$$ka = \frac{2 \cdot \pi \cdot a}{\lambda} \tag{4}$$

Scattering of structures smaller than the wavelength ($ka << 1$) is characterized by an exponential intensity increase with increasing ka (Rayleigh scattering), whereas the intensity for ka-values of one and higher is fluctuating due to interference of structure and wavelength (Mie scattering) (Fig. 3). This means that in the Rayleigh-scattering domain, within a finite frequency bandwidth, the scatterer size inversely correlates to the spectral amplitude increase with increasing frequency. In addition to the scatterer size, its shape, orientation and acoustic impedance mismatch to the surrounding medium impact the scattering intensity emitted in any given direction. Altogether, the following implications derive from the use of higher ultrasound frequencies: 1) Spatial resolutions are increased but also the acoustic attenuation. 2) The sensitivity towards scatterers with a certain dimension much smaller than the wavelength increases by an increase of the ka-value.

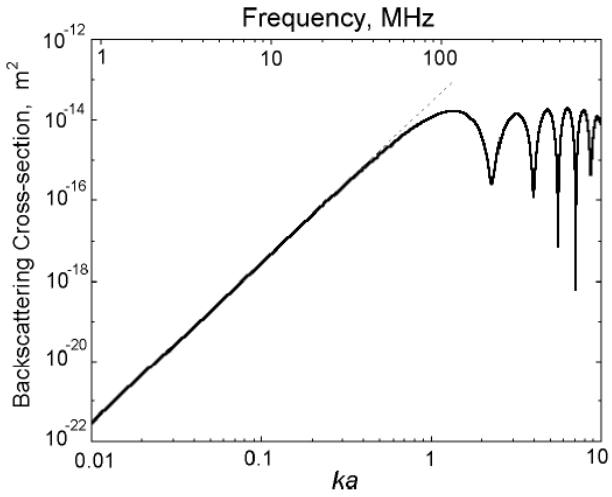

Figure 3: Backscatter intensity as a function of the ka-value and frequency under the assumption of a constant effective scatterer size of 2.7 µm. Note the exponential increase in the Rayleigh scattering domain for ka-values significantly smaller than 1. Reprinted from [14], Fig. 5.4, with permission from Oxford University Press.

For tissue characterization, backscatter intensity of incoherent scattering can be modeled for various shapes, orientations and elastic scatterer properties by theoretical backscatter spectra. Using a 3D spatial autocorrelation function, the following closed-form solution was derived:

$$W_{theor}(f) = B(L,q) \cdot C(a_{eff}, n_z) \cdot f^4 \cdot F(f, a_{eff}), \tag{5}$$

with a_{eff} being the effective scatterer size, C the scattering strength, and n_z the average acoustic concentration, the latter being derived from the product of number density and acoustic impedance difference between medium and scatterer. $B(L,q)$ accounts for source

and windowing characteristics given a gate length L and a transducer focal parameter q. F denotes the form factor that in the case of randomly distributed spherical scatterers is dependent only on frequency and the effective scatterer size. Numerous form factors were proposed to model the scattering specifically for cells, such as the Gaussian form factor that models a continuous spatial change of acoustic impedance between medium and scatterer. The comparison between a measured spectrum and theoretical spectra derived for different effective scatterer sizes then enables an estimate of the effective scatterer size of the measured volume. The underlying data processing steps vastly differ from conventional B-mode imaging (Fig. 4).

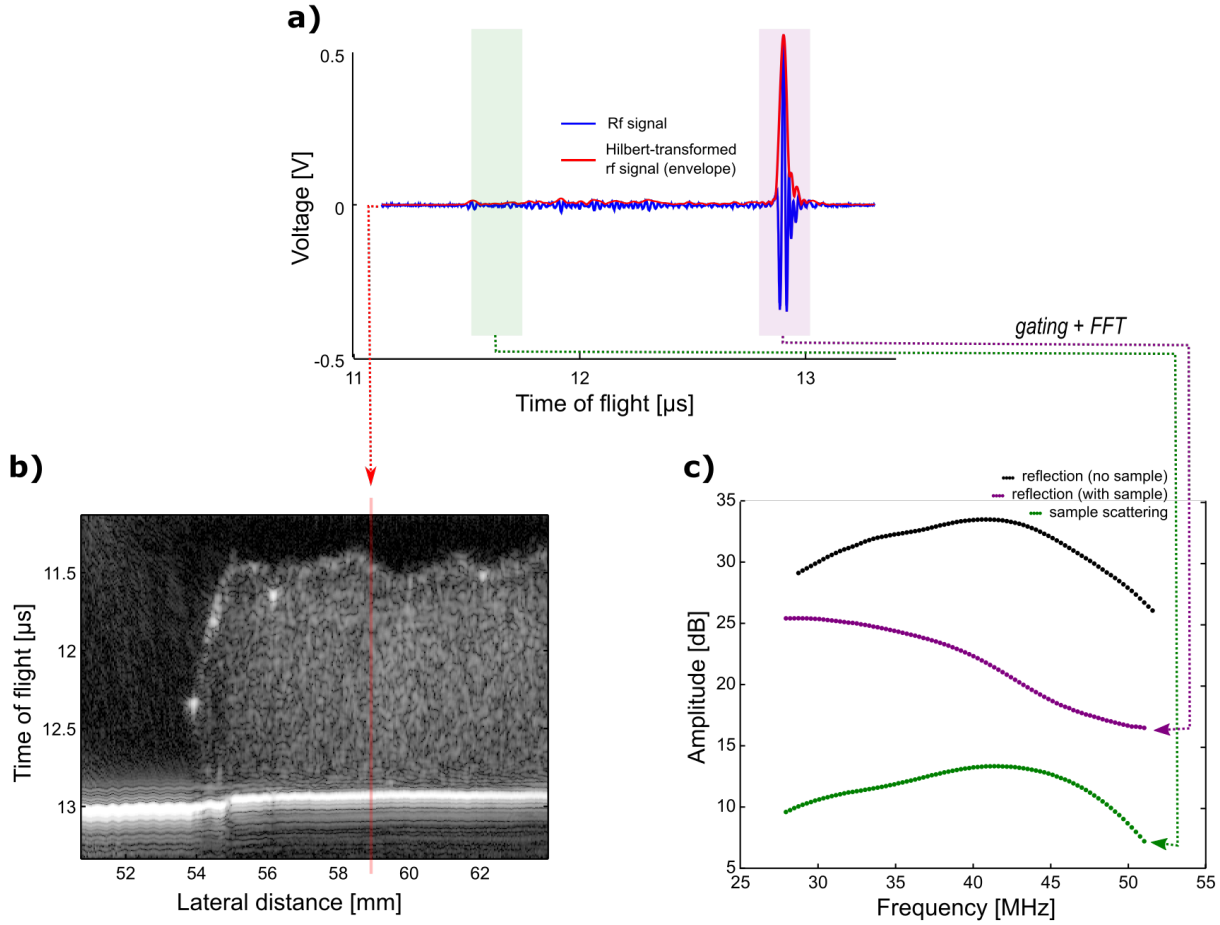

Figure 4: Different usage of the radio frequency (rf) signals for conventional ultrasound imaging and quantitative ultrasound. (a): Received rf signals and Hilbert-transformed (signal envelope) of a single pulse echo signal. (b): Conventional B-mode image with the signal envelope as one line (c): Windowing, gating and Fast Fourier Transform (FFT) of the rf-data provides ultrasound spectra used for quantitative ultrasound. Comparing the reflection of a glass plate (visible in B-mode image as bright band at the bottom) with and without overlaying tissue sample, frequency-dependent differences are visible that are due to acoustic attenuation. Moreover, spectra obtained from the sample (green color) are shifted towards higher frequencies. This example highlights that spectral analysis of ultrasound rf-data provides access to information that cannot be reconstructed from conventional B-mode images.

Theoretical formulations [15] and experimental applications have been conducted to suc-

cessfully utilize quantitative backscatter parameters for various tissue characterizations, *e.g.* thyroid cancer [16], ocular tumors [17], or differentiation between mammary fibroadenomas, sarcomas and carcinomas [18].

For cartilage tissue, the incorporation of spectral features other than integrated amplitude had not yet been achieved. One reason is that the estimation of spectra requires locally homogeneous scattering properties in the direction of sound propagation with axial dimensions in the order of several pulse lengths. However, these requirements cannot be met in cartilage tissue. Its layered structure consists of three distinct layers, in which cells and collagen fibrils gradually change geometry, density, and orientation, which results in gradual changes of acoustic backscatter and bulk properties, *e.g.* speed of sound and attenuation [19]. This inhomogeneity prevents an easy transfer of established backscatter signal processing and parameters to cartilage.

The most common and established ultrasound parameters to assess articular cartilage are surface reflection amplitude and surface roughness as surrogates for alterations of cartilage matrix stiffness and roughness, respectively. These parameters tend to be sensitive to the degenerative stage of the cartilage, and results are accurate if the local inclination with respect to the ultrasound propagation direction can be controlled [20]. As in the case of surface reflection intensity, the subchondral bone boundary intensity was shown to vary in the course of OA due in some part to changes of bone density, of trabecular thickness in the subchondral bone tissue and of acoustic attenuation of the cartilage matrix [21].

In addition to the assessment of meaningful ultrasound parameters from the cartilage surface and subchondral bone boundary, parameters measured from cartilage extracellular matrix could further enhance the diagnostic potential of ultrasound to detect different cartilage degeneration stages. The most commonly derived parameter is the apparent integrated backscatter (AIB) that quantifies the mean backscattered energy within the frequency bandwidth of the transducer, as proposed twenty years ago by Cherin et al. [22]. Large changes of AIB were observed during ageing [23] and between fibrous and hyaline-like cartilage repair tissue [24]. However, the effectiveness of this parameter in distinguishing different OA degeneration levels appears limited for samples with spontaneous OA [25] and enzymatically degraded cartilage [26]. Nevertheless, quantitative ultrasound may offer enhanced sensitivities by providing parameters, that analyze the frequency-dependence of backscattered ultrasound spectra rather than only the integrated amplitude.

The hypothesis of this work is that cartilage extracellular matrix degeneration affects the backscattered ultrasound spectrum, thereby allowing spectral parameters to be distinguishing features between healthy and degenerated cartilage. Furthermore, we suggest that this relationship has remained unidentified due to the implicit removal of frequency-dependent changes in the AIB-calculation, which has thus far been the backscatter feature used for detecting OA-related extracellular changes. The primary aims of this work are therefore:

- To identify and establish signal processing methods for a spectrum estimation that is suitable for the complex structure of hyaline cartilage and does not violate the condition of local homogeneity (Study A).
- To analyze the diagnostic value of the frequency-dependence of backscattered signals and envelope statistics parameters in characterizing OA (Study A).
- To combine the diagnostic potential of ultrasound surface and backscatter parameters by selecting relevant features with respect to different degeneration stages and employing them in classification and receiver operating characteristics (ROC) analyses (Study B).
- To model the integrated backscatter amplitude as a function of collagen amount, proteoglycan amount and cell-number density in order to identify those structural components that influence the backscattered signal in the extracellular matrix of hyaline cartilage in a quantitative manner (Study C).

2 Materials and Methods

2.1 Samples

Studies A and B used biopsies of human hyaline cartilage obtained from the femoral condyles during alloplastic implant surgery ($N = 38$) and from donors with no degenerative joint disease ($N = 10$). Study C used osteochondral cylinders of cartilage obtained from patellae of human ($N = 16$), bovine ($N = 8$) and ovine ($N = 10$) origin. Human donor ages were in the range from 24-92 years. Samples of bovine and ovine origin were obtained at estimated animal ages of 1-3 and 1-8 years, respectively. Approval for the experiments was granted from the ethics commissions and approved by local institutional review boards.

2.2 Ultrasound measurements

All cartilage measurements were performed in time-resolved C-scan mode, *i.e.* the ultrasound probe scanned a grid parallel to the surface of the specimen. All samples were scanned using a spherically focused 40 MHz single element transducer. The entire biopsy was measured in all studies, and are denoted as full-biopsy measurements. Additionally, in Study C, one central cross-section (thickness: 750 µm) was prepared and measured for each osteochondral cylinder immediately after measurement of the full biopsy. In the following, these measurements are referred to as cross-section measurements.

2.3 Structural parameters

In study A/B, the primary focus was the assessment of the degenerative state of cartilage for the respective biopsies. Cartilage degeneration was assessed using the individual scoring categories of the 14-point Mankin-score. Of particular interest were the structure score and the scoring of cellular abnormalities, referred to as Mankin I and Mankin II, respectively. Moreover, the cells were counted in one histological section in a 1 mm 2 square area directly below the cartilage surface. In study C, the primary focus was the quantitative and directional assessment of four main components of the extracellular cartilage matrix, *i.e.* collagen- and proteoglycan-concentrations, collagen orientation and cell number density. Collagen and proteoglycan-concentrations were estimated by Fourier-transform infrared imaging spectroscopy (FT-IRIS) measurements of the cartilage cross-sections at a spatial resolution of 25 µm. Three repeated scans were performed and averaged for each specimen. Collagen orientation was estimated by polarized light microscopy (PLM) of the cartilage cross-sections using stokes parameters at 0°, 45°and 90°. The cell number density was estimated from light microscope images of histological sections stained with Safranin-O. All four parameters were averaged into 15 depth-dependent regions of interest (ROI) for every sample to enable subsequent site-matched analyses with ultrasound parameters.

2.4 Ultrasound data analysis

To estimate a meaningful ultrasound backscatter spectrum, the following signal processing steps are typically performed: (a) definition of a region of interest in both axial (time-windows) and lateral (adjacently acquired pulse-echoes) direction, (b) multiplication of time windows with a gating function, for all pulse-echoes of interest (c), calculation of the FFT of the gated windows to obtain the backscatter spectra $S_m(k)$, (d) correction of $S_m(k)$ with a time-of-flight matched spectrum of a reference material measurement $S_{ref}(k)$ to derive the normalized backscatter spectra, and (e) averaging spectra in the lateral direction to obtain the normalized, averaged backscatter power spectrum $W(f)$. In study A, three major modifications from standard signal processing routines were established:

(1) Very short time gates were used to account for the depth-dependent gradual change of acoustic and morphological parameters of the cartilage matrix. To countermeasure the resulting inaccuracies of the estimated spectrum, the averaging over several pulse-echoes, *i.e.* lateral averaging, had to be considerably increased. However, due to the natural curvature of the cartilage surface, the expansion of the regions of interest in the lateral direction likely violates the constraint of local homogeneity during averaging of different pulse-echoes. Hence, the idea was to determine the gate limits for every pulse-echo with respect to a previously calculated surface time delay resulting in regions of interest that are shaped exactly like the surface, but at higher cartilage depths. By doing so, at the cost of lateral resolution, the axial resolution of the estimated spectra could be significantly increased, at

the cost of lateral resolution.

(2) Typically, especially for lower-frequency transducers, time-of-flight matched spectra from planar reflectors are used to compensate for the loss of pressure amplitude and diffraction effects at defocused positions. However, we have observed significant phase interference artifacts for defocused planar reflections for the applied transducer (see Appendix 2 in study A). As an alternative, a sample containing finely powdered graphite particles immersed in agar was used as a reference material to better mimic the mean amplitude decrease for defocused positions for scattering particles. Note that in this approach diffraction effects were neglected in studies A/B, whereas in study C, the diffraction effects were included in the reference spectra through calculation of frequency-dependent deviations of defocused spectra from the confocal spectrum of the agar-graphite phantom.

(3) Prior to calculation of the FFTs, the surface reflection of the rf-signal was gated out by adding the inverted Tukey-window (length 2.5 PL, α= 0.5) at the surface position. By doing so, a strict differentiation of backscattered signals from the specular surface reflection was achieved and meaningful spectra from the superficial cartilage zone could be estimated.

The normalized average backscatter power spectra $W(f)$ were used to estimate two different parameters: (a) the conventional apparent integrated backscatter AIB and (b) the apparent frequency dependence of backscatter AFB, *i.e.* the spectral slope calculated by linear regression analysis of the frequency-dependence of backscatter amplitude within the transducer bandwidth. Both parameters were calculated as a function of tissue depth, from which in total six single parameters were derived (Table 2).

Table 2: Derived amplitude and spectral slope parameters from depth-dependent spectra. †: derived by linear regression analysis with minimum starting depth 0.3 mm. AIB and AFB refer to integrated amplitude and spectral slope values, respectively.

Parameter	Unit	Parameter explanation	Study
AIB_{max}	dB	Maximum AIB between surface and 0.3 mm depth	A,B,C
AFB_{max}	$\frac{dB}{MHz}$	Maximum AFB between surface and 0.3 mm depth	A,B
$AIB^{\dagger}_{slope}$	$\frac{dB}{mm}$	Depth-dependent decrease of AIB	A,B
$AFB^{\dagger}_{slope}$	$\frac{dB}{mmMHz}$	Depth-dependent decrease of AFB	A
$AIB^{\dagger}_{0}$	dB	Extrapolated value of AIB-slope to cartilage surface	A,B
$AFB^{\dagger}_{0}$	$\frac{dB}{MHz}$	Extrapolated value of AFB-slope to cartilage surface	A

2.5 Statistics

Study A assessed differences of the backscatter and envelope statistics parameters with respect to degeneration of cartilage surface and extracellular matrix, given by Mankin score I and Mankin score II, respectively, by one-way Kruskal-Wallis non-parametric analyses of variance. Post hoc multiple comparison Tukey tests were carried out to identify differences

among sub-groups. Correlations between AIB and cell number density were analyzed using Pearsons correlation and R^2 values were provided as measures for goodness of the fits.

Study B employed feature selection and classification algorithms to study the prediction potential of a combination of ultrasound surface, backscatter and envelope statistics parameters with respect to different degeneration stages. Six binary classifications were carried out to distinguish the samples at each degeneration level. The degeneration level was defined as the sum of Mankin I and Mankin II. Quasi-least squares regressions (QLS) were carried out with all combinations of two ultrasound parameters as predictors for all binary classifications, followed by receiver operating characteristics (ROC) analysis for the parameter pairs attaining the highest classification accuracy. The best ultrasound parameter pair for the distinction of all degeneration states was determined by the highest area under the curve value (AUC) of the ROC analysis.

Study C modeled the backscatter amplitude (target variable) by cell number density and concentrations of proteoglycan and collagen (predictor variables). Only regions of cross-section measurements with the average collagen orientation being approximately perpendicular to the sound beam axis were included. Analyses were performed for the individual predictor variables and with all combinations of the three predictor variables (multivariate regression). Provided were p-values, intercept and regression coefficients, 95% confidence intervals and partial correlation coefficients. In all studies, results were considered significant for $p < 0.05$.

3 Results

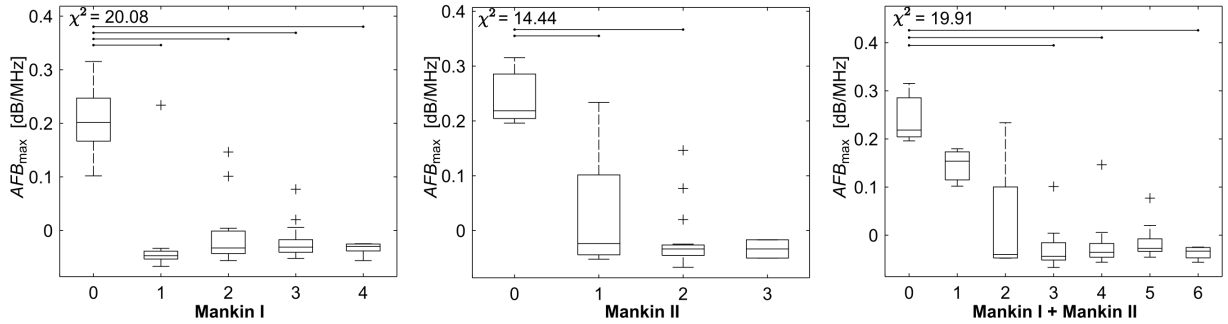

Figure 5: Box plots of the spectral slope value AFB_{max} with respect to the cartilage degeneration scores of (a), the structure and surface (Mankin I), (b), the degeneration score of the extracellular matrix (Mankin II) and (c), the cumulative Mankin score. Horizontal lines indicate statistically significant differences between the degeneration scores.

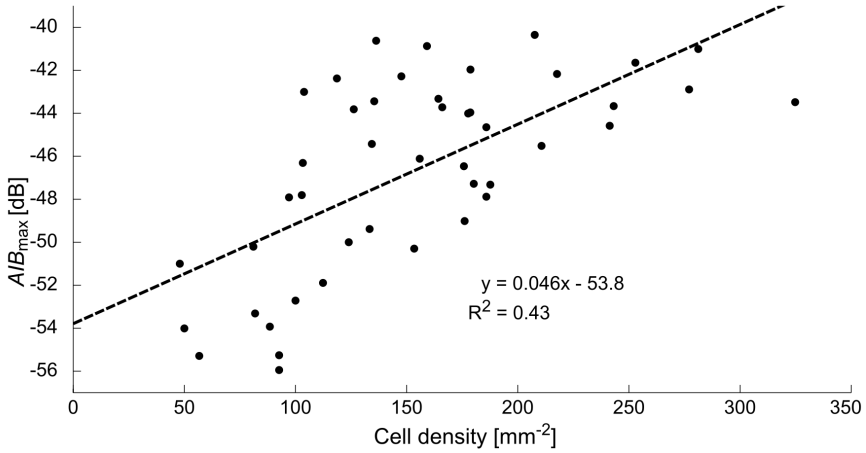

Figure 6: Scatter plot of cell number density versus integrated backscatter amplitude AIB of study A. The dotted line represents the linear regression curve.

Spectral slope parameters exhibit highest sensitivities towards cartilage degeneration. Statistically significant differences were particularly observed in the maximum spectral slope value of the superficial cartilage zone, with respect to degeneration scores. Multi-comparison tests revealed that the spectral slope value for non-degenerated cartilage was significantly higher compared to degenerated cartilage for structure and matrix degeneration, respectively. Particularly, we observed a spectral peak between 40-50 MHz for healthy cartilage samples, that disappeared for all samples with mild or moderate signs of degeneration. In contrast, the backscatter amplitude exhibited no significant differences with respect to cartilage matrix degeneration and lower significance levels between later stage degenerations with respect to cartilage structure degeneration (Fig. 5).

Cell number density and ultrasound backscatter amplitude are moderately correlated. Linear regression analysis revealed a statistically significant positive correlation between cell number density and integrated backscatter amplitude of all human samples with variable degeneration states ($R^2 = 0.43$) in study A (Fig. 6). In study C, including three different species in the linear regression analysis, a similar coefficient of determination ($R^2 = 0.41$) was observed for the correlation between cell number density and ultrasound backscatter intensity.

Combinations of ultrasound parameters exhibit potential to discriminate between different, particularly very early, degeneration stages.
The best classification accuracies and AUC-values of the ROC analyses were obtained for discrimination between Mankin scores 0 and 1 and between Mankin score 1 and 2 (AUC = 0.99). Accuracy and AUC-values decreased for discriminations of later stage degenerations. Feature selection demonstrated that envelope statistics and surface parameters were feature candidates throughout all degeneration stages, whereas backscatter spectral slope and backscatter amplitude were selective for early (Fig. 7 a,b) and advanced degeneration stages (Fig. 7 c), respectively.

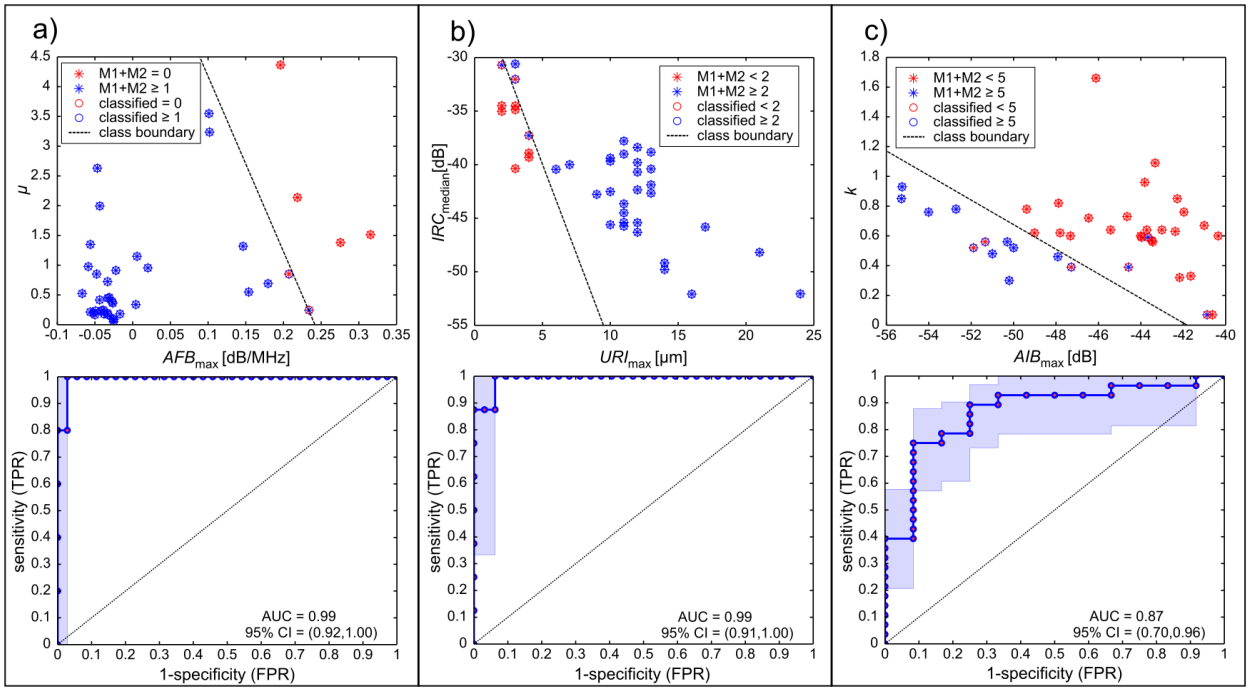

Figure 7: Class plots (upper panel) with the best performing ultrasound parameter pairs and the corresponding ROC curves (lower panel) for an excerpt of 3 Mankin subset score classifications. The positive (red data points) and negative (blue) class labels represent lower and higher Mankin scores, respectively. Classification output is highlighted by circles in blue and red, the class boundaries are indicated by black dashed lines.

Variations of ultrasound backscatter amplitude are related to natural variations of collagen concentration and cell number density.

Linear regression analysis revealed a positive relationship ($R^2 = 0.51$) of backscatter amplitude derived from cartilage cross sections with a 2D model of site-matched estimates of cell number density and collagen concentration (Fig. 8). Both regression coefficients were positive, highlighting that increased cell number density or collagen concentrations are expected to result in increased backscatter amplitudes. In comparison, the proteoglycan concentration showed an inferior impact on ultrasound backscatter amplitude. The partial correlation coefficients suggested a similar contribution of cell number density and collagen to ultrasound backscatter.

4 Discussion

Study A showed that spectral and envelope statistical parameters are sensitive to osteoarthritic changes, particularly early degenerative changes. In contrast, amplitude-based parameters, *i.e.* the AIB, which up to the present time have been used as indicators for cartilage matrix degenreation, showed little or no statistically significant differences with respect to different degeneration stages. This finding was surprising since the spectral and envelope statistics parameters were newly proposed in this study.

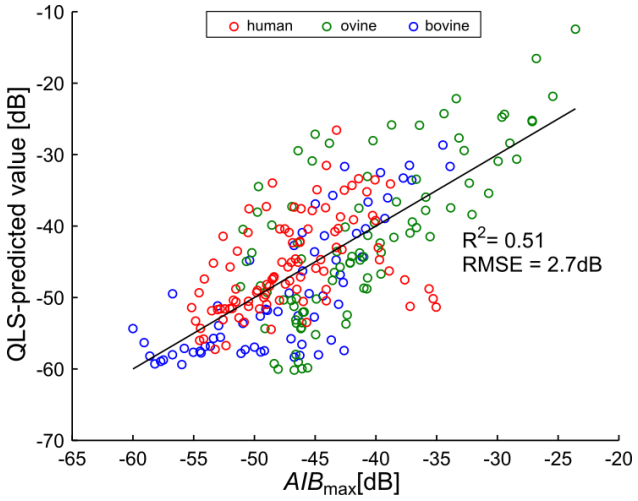

Figure 8: Scatter plot of backscatter intensity versus the backscatter intensity value modeled by a multivariate QLS model using site-matched linearized collagen quantity and cell number density as predictor variables.

As confirmed by study C, more than 50% of the backscatter amplitude can be attributed to the natural variations of collagen quantity and cell number density in healthy cartilage. This relationship alone suggests that the AIB should decrease with higher cartilage degenerations since these constituents are known to decrease with disease progression. However, counter-evidence is the lack of statistically significant differences of the AIB with respect to the Mankin score. This discrepancy can be attributed to concurrent structural changes of the cartilage matrix and cartilage surface in the course of degeneration. For example, the AIB may be concurrently increased by reduced collagen packing density in fibrous cartilage repair tissue [24], through additional acoustic interfaces due to the formation of cracks in later stage degenerations [27], a decrease of acoustic attenuation of the cartilage matrix [28], or a reduction of acoustic impedance [29], resulting in a reduction of the specular surface reflection and thereby higher acoustic pressure amplitudes within the cartilage matrix. These processes and their impact on the backscatter amplitude highlight that the interpretation of AIB is extremely challenging, particularly in the scope of predicting different cartilage degeneration stages.

Hence, additional parameters containing information about the structural integrity of the cartilage matrix are needed to put the AIB into context. Potential ultrasound parameters that could fulfill this task are spectral and envelope statistics parameters due to their sensitivity to micro-structural, sub-wavelength structures. The statistical differences with respect to different degeneration stages provided in study A highlighted this potential and inspired the idea to use combinations of ultrasound parameters to predict the different degeneration stages of study B. The outcome of this study was that with just two parameters as predictor variables, a very good classification between different degeneration stages, particularly the earliest ones, was possible. Moreover, the feature selection highlighted that

surface and envelope statistics parameters are potential feature candidates to discriminate between all degeneration stages, whereas the spectral amplitude and the spectral slope were suitable features for late and early degeneration discriminations, respectively. The choice of two predictor variables was necessary to accommodate the relatively low sample number and to prevent overfitting of the data. We anticipate that the provided classification performance can be further improved by incorporating more than two predictor variables into the models or by using a more complex statistical model than linear regression analysis. It is probable, that a full discrimination between different degeneration stages with ultrasound parameters would then become possible.

However, even though evidence was provided that ultrasound can in principle be used to distinguish between different degeneration stages, clinical impact remained limited. This can be primarily attributed to the fact that the connection between ultrasound parameters and underlying structural components was still missing. The major motivation to conduct study C was to fill this gap, and within the framework of this study we could demonstrate that the main structural components that contribute to US backscatter at this frequency range are collagen and chondrocytes. However, study C could not definitely identify the structures contributing to the observed frequency-dependence of backscatter in healthy cartilage. Nevertheless, the data analyses of this study has led to a promising hypothesis:

In principle, the observed frequency-dependence indicates changes in the size or spatial arrangement of the scatterers. Cell size and spacing in the direction perpendicular to the surface is known to be fairly regular in intact cartilage [30] but this regularity can be lost during degeneration, *e.g.* by fibrillation, hyper- or hypocellularity, or morphological changes of collagen. We hypothesize that the narrow-band peak in the spectrum observed in all experiments is caused by coherent scattering from more or less periodically arranged cell layers. A disappearance of the spectral peak would then indicate loss of structural periodicity due to tissue degeneration. The in-depth analysis of position, amplitude and width of coherent scattering may be a novel indicator of the integrity and regularity of the superficial cartilage zone. In a very recent study, Rohrbach et al. could confirm this hypothesis and furthermore demonstrated a strong correlation between the chondrocyte layer spacing and the pronounced frequency peak [31].

Another limitation on the clinical impact is related to the pending application of the introduced ultrasound parameters *in vivo*. The presented studies investigated cartilage samples *ex vivo* and effects of surface inclination, medium attenuation, additional acoustic interfaces and transducer-sample distances could be effectively controlled. Nevertheless, from a technical perspective, an i*n vivo* application is straightforward, particularly for minimally invasive arthroscopic ultrasound, since this has already been successfully applied and an AIB at a similar ultrasound frequency range could be determined in numerous studies. Other features like the spectral slope, amplitude differences between different frequency bandwidths

or envelope statistics parameters can easily be added to these investigations. However, before application, robustness and accuracy of the spectral parameters should be verified for the IVUS-transducers, since spectral differences may falsely occur, *e.g.* due to diffraction, frequency-dependent attenuation of the medium or inaccurate reference measurements.

In conclusion, this work demonstrated for the first time that envelope statistics and spectral slope parameters are sensitive to early stages of extracellular matrix degeneration and outperform conventionally used amplitude-based parameters. The sensitivity has been confirmed by a feature selection and classification approach, that has also revealed that spectral slope parameters are particularly sensitive to early degenerative changes of the extracellular cartilage matrix. Moreover, this work has shown for the first time that chondrocytes and collagen are a major scattering source in hyaline cartilage and contribute to approximately 50% of the ultrasound backscatter intensity at the applied frequency range of 25-50 MHz. However, this work could only speculate about the structural origin for the amplitude peaks at ultrasound frequencies between 40 and 50 MHz in healthy cartilage, an issue that is now the focus of a promising study by Rohrbach et al. who showed that this peak can be attributed to the chondrocyte layer spacing [31]. The understanding of ultrasound scattering still requires further investigation in future studies to enable a successful clinical application of cartilage matrix degeneration classification using high-frequency ultrasound.

5 References

[1] D. Pereira, B. Peleteiro, J. Araujo, J. Branco, R. A. Santos, and E. Ramos, "The effect of osteoarthritis definition on prevalence and incidence estimates: a systematic review," *Osteoarthritis.Cartilage.*, vol. 19, pp. 1270–1285, Nov. 2011.

[2] D. T. Felson, R. C. Lawrence, P. A. Dieppe, R. Hirsch, C. G. Helmick, J. M. Jordan, R. S. Kington, N. E. Lane, M. C. Nevitt, Y. Zhang, M. Sowers, T. McAlindon, T. D. Spector, A. R. Poole, S. Z. Yanovski, G. Ateshian, L. Sharma, J. A. Buckwalter, K. D. Brandt, and J. F. Fries, "Osteoarthritis: new insights. part 1: the disease and its risk factors," *Ann.Intern.Med.*, vol. 133, pp. 635–646, Oct. 2000.

[3] N. Männicke, M. Schöne, M. Gottwald, F. Göbel, M. L. Oelze, and K. Raum, "3-d high-frequency ultrasound backscatter analysis of human articular cartilage," *Ultrasound Med Biol*, vol. 40, pp. 244–257, Jan. 2014.

[4] K. P. Pritzker, S. Gay, S. A. Jimenez, K. Ostergaard, J. P. Pelletier, P. A. Revell, D. Salter, and W. B. van den Berg, "Osteoarthritis cartilage histopathology: grading and staging," *Osteoarthritis.Cartilage*, vol. 14, pp. 13–29, Jan. 2006.

[5] H. J. Mankin, H. Dorfman, L. Lippiello, and A. Zarins, "Biochemical and metabolic abnormalities in articular cartilage from osteo-arthritic human hips. ii. correlation of

morphology with biochemical and metabolic data," *J.Bone Joint Surg.Am.*, vol. 53, pp. 523–537, Apr. 1971.

[6] A. Guermazi, D. Hayashi, F. Eckstein, D. J. Hunter, J. Duryea, and F. W. Roemer, "Imaging of osteoarthritis," *Rheum.Dis.Clin.North Am.*, vol. 39, pp. 67–105, Feb. 2013.

[7] Y. Wang, A. J. Teichtahl, and F. M. Cicuttini, "Osteoarthritis year in review 2015: imaging," *Osteoarthritis.Cartilage.*, vol. 24, pp. 49–57, Jan. 2016.

[8] M. D. Crema, F. W. Roemer, M. D. Marra, D. Burstein, G. E. Gold, F. Eckstein, T. Baum, T. J. Mosher, J. A. Carrino, and A. Guermazi, "Articular cartilage in the knee: current mr imaging techniques and applications in clinical practice and research," *Radiographics*, vol. 31, pp. 37–61, Jan. 2011.

[9] D. T. Felson, "Arthroscopy as a treatment for knee osteoarthritis," *Best.Pract.Res.Clin.Rheumatol.*, vol. 24, pp. 47–50, Feb. 2010.

[10] P. Kiviranta, E. Lammentausta, J. Toyras, I. Kiviranta, and J. S. Jurvelin, "Indentation diagnostics of cartilage degeneration," *Osteoarthritis.Cartilage.*, vol. 16, pp. 796–804, July 2008.

[11] T. Viren, S. Saarakkala, E. Kaleva, H. J. Nieminen, J. S. Jurvelin, and J. Toyras, "Minimally invasive ultrasound method for intra-articular diagnostics of cartilage degeneration," *Ultrasound Med.Biol.*, vol. 35, pp. 1546–1554, Sept. 2009.

[12] J. Liukkonen, P. Lehenkari, J. Hirvasniemi, A. Joukainen, T. Viren, S. Saarakkala, M. T. Nieminen, J. S. Jurvelin, and J. Toyras, "Ultrasound arthroscopy of human knee cartilage and subchondral bone in vivo," *Ultrasound Med.Biol.*, vol. 40, pp. 2039–2047, Sept. 2014.

[13] E. Kaleva, T. Viren, S. Saarakkala, J. Sahlman, J. Sirola, J. Puhakka, T. Paatela, H. Kröger, I. Kiviranta, J. S. Jurvelin, and J. Töyräs, "Arthroscopic ultrasound assessment of articular cartilage in the human knee joint," *Cartilage*, vol. 2, pp. 246–253, July 2011.

[14] R. S. C. Cobbold, *Foundations of biomedical ultrasound*. Oxford University Press, 2006.

[15] M. F. Insana and T. J. Hall, "Parametric ultrasound imaging from backscatter coefficient measurements: image formation and interpretation," *Ultrason.Imaging*, vol. 12, pp. 245–267, Oct. 1990.

[16] R. J. Lavarello, W. R. Ridgway, S. S. Sarwate, and M. L. Oelze, "Characterization of thyroid cancer in mouse models using high-frequency quantitative ultrasound techniques," *Ultrasound Med.Biol.*, vol. 39, pp. 2333–2341, Dec. 2013.

[17] F. L. Lizzi, M. Astor, T. Liu, C. Deng, D. J. Coleman, and R. H. Silverman, "Ultrasonic spectrum analysis for tissue assays and therapy evaluation," vol. 8, no. 1, pp. 3–10, 1997.

[18] M. L. Oelze and J. O'Brien, W.D., "Application of three scattering models to characterization of solid tumors in mice," *Ultrason.Imaging*, vol. 28, pp. 83–96, Apr. 2006.

[19] D. H. Agemura, J. O'Brien, W.D., J. E. Olerud, L. E. Chun, and D. E. Eyre, "Ultrasonic propagation properties of articular cartilage at 100 MHz," *J.Acoust.Soc.Am.*, vol. 87,

pp. 1786–1791, Apr. 1990.

[20] M. Schöne, N. Männicke, M. Gottwald, F. Göbel, and K. Raum, "3-d high frequency ultrasound improves the estimation of surface properties in degenerated cartilage," *Ultrasound Med.Biol.*, vol. 39, pp. 834–844, May 2013.

[21] S. Saarakkala, S. Z. Wang, Y. P. Huang, J. S. Jurvelin, and Y. P. Zheng, "Characterization of center frequency and bandwidth of broadband ultrasound reflected by the articular cartilage to subchondral bone interface," *Ultrasound Med.Biol.*, vol. 37, pp. 112–121, Jan. 2011.

[22] E. Cherin, A. Saied, P. Laugier, P. Netter, and G. Berger, "Evaluation of acoustical parameter sensitivity to age-related and osteoarthritic changes in articular cartilage using 50-mhz ultrasound," *Ultrasound Med.Biol.*, vol. 24, pp. 341–354, Mar. 1998.

[23] B. Pellaumail, A. Watrin, D. Loeuille, P. Netter, G. Berger, P. Laugier, and A. Saied, "Effect of articular cartilage proteoglycan depletion on high frequency ultrasound backscatter," *Osteoarthritis.Cartilage.*, vol. 10, pp. 535–541, July 2002.

[24] K. Gelse, A. Olk, S. Eichhorn, B. Swoboda, M. Schoene, and K. Raum, "Quantitative ultrasound biomicroscopy for the analysis of healthy and repair cartilage tissue," *Eur.Cell Mater.*, vol. 19, pp. 58–71, 2010.

[25] H. J. Nieminen, Y. Zheng, S. Saarakkala, Q. Wang, J. Toyras, Y. Huang, and J. Jurvelin, "Quantitative assessment of articular cartilage using high-frequency ultrasound: research findings and diagnostic prospects," *Crit Rev.Biomed.Eng*, vol. 37, no. 6, pp. 461–494, 2009.

[26] S. Z. Wang, Y. P. Huang, S. Saarakkala, and Y. P. Zheng, "Quantitative assessment of articular cartilage with morphologic, acoustic and mechanical properties obtained using high-frequency ultrasound," *Ultrasound Med.Biol.*, vol. 36, pp. 512–527, Mar. 2010.

[27] S. L. Myers, K. Dines, D. A. Brandt, K. D. Brandt, and M. E. Albrecht, "Experimental assessment by high frequency ultrasound of articular cartilage thickness and osteoarthritic changes," *J.Rheumatol.*, vol. 22, pp. 109–116, Jan. 1995.

[28] H. J. Nieminen, S. Saarakkala, M. S. Laasanen, J. Hirvonen, J. S. Jurvelin, and J. Toyras, "Ultrasound attenuation in normal and spontaneously degenerated articular cartilage," *Ultrasound Med.Biol.*, vol. 30, pp. 493–500, Apr. 2004.

[29] S. Leicht and K. Raum, "Acoustic impedance changes in cartilage and subchondral bone due to primary arthrosis," *Ultrasonics*, vol. 48, pp. 613–620, Nov. 2008.

[30] K. D. Jadin, W. C. Bae, B. L. Schumacher, and R. L. Sah, "Three-dimensional (3-d) imaging of chondrocytes in articular cartilage: growth-associated changes in cell organization.," *Biomaterials*, vol. 28, pp. 230–9, Jan 2007.

[31] D. Rohrbach, S. I. Inkinen, J. Zatloukalová, A. Kadow-Romacker, A. Joukainen, M. K. Malo, J. Mamou, J. Toyras, and K. Raum, "Regular chondrocyte spacing is a potential cause for coherent ultrasound backscatter in human articular cartilage," *J.Acoust.Soc.Am.*, vol. 141, no. 5, pp. 3105–3116, 2017.

Eidesstattliche Versicherung

„Ich, Nils Stefan Männicke, versichere an Eides statt durch meine eigenhändige Unterschrift, dass ich die vorgelegte Dissertation mit dem Thema: "High-frequency ultrasound backscatter analysis of hyaline cartilage" selbstständig und ohne nicht offengelegte Hilfe Dritter verfasst und keine anderen als die angegebenen Quellen und Hilfsmittel genutzt habe.
Alle Stellen, die wörtlich oder dem Sinne nach auf Publikationen oder Vorträgen anderer Autoren beruhen, sind als solche in korrekter Zitierung (siehe „Uniform Requirements for Manuscripts (URM)" des ICMJE -*www.**icmje**.org*) kenntlich gemacht. Die Abschnitte zu Methodik (insbesondere praktische Arbeiten, Laborbestimmungen, statistische Aufarbeitung) und Resultaten (insbesondere Abbildungen, Graphiken und Tabellen) entsprechen den URM (s.o) und werden von mir verantwortet.
Meine Anteile an den ausgewählten Publikationen entsprechen denen, die in der untenstehenden gemeinsamen Erklärung mit dem/der Betreuer/in, angegeben sind. Sämtliche Publikationen, die aus dieser Dissertation hervorgegangen sind und bei denen ich Autor bin, entsprechen den URM (s.o) und werden von mir verantwortet.
Die Bedeutung dieser eidesstattlichen Versicherung und die strafrechtlichen Folgen einer unwahren eidesstattlichen Versicherung (§156,161 des Strafgesetzbuches) sind mir bekannt und bewusst."

Datum Unterschrift

Anteilserklärung an den erfolgten Publikationen

Nils Stefan Männicke hatte folgenden Anteil an den folgenden Publikationen:

Publikation 1: Männicke N, Schöne M, Gottwald M, Göbel F, Oelze ML, Raum K: 3-D High-Frequency Ultrasound Backscatter Analysis of Human Articular Cartilage. Ultrasound in Medicine and Biology, Jan 2014.

80%
Beitrag im Einzelnen:
Maßgeblich verantwortlich für Planung der Auswertung der bereits vorliegenden Daten
Einleitung / Methodik / Ergebnisse:

- Entwicklung und Implementierung der vollständigen Signalverarbeitungskette in Matlab (Ausnahme: Approximation der Knorpeloberfläche in gemeinsamer Implementierung mit Martin Schöne)
- Anpassung/Optimierung der etablierten Rückstreusignalauswertungsroutinen, insbesondere die Verwendung von short time gate FFTs und angepasster Regions of Interest sowie Verwendung alternativer physikalischer Phantome (Agar-Graphit) zur Bestimmung der Referenzspektra
- Berechnung der entwickelten Parameter (Ausnahme: Oberflächenparameter übernommen aus Studie von Martin Schöne)
- Durchführung der statistischen Auswertung

Diskussion:

- Interpretation und Diskussion der entwickelten Methodik und der gewonnenen Daten (mit fachlicher Unterstützung von Prof. Dr. Kay Raum) und Diskussion mit Ko-Autoren

Manuskript:

- Grafische Aufarbeitung der Ergebnisse (Ausnahme: Fig. 1 erstellt durch Martin Schöne)
- Initialer Entwurf des gesamten Manuskripts und eigenständige Überarbeitung auf Basis der Begutachtungen der Ko-Autoren und im Rahmen des Review-Prozesses

Publikation 2: Männicke N, Schöne M, Oelze,ML, Raum,K: Articular cartilage degeneration classification by means of high-frequency ultrasound. Osteoarthritis Cartilage, Okt 2014.

80%

Beitrag im Einzelnen:

Maßgeblich verantwortlich für Planung der Auswertung der bereits vorliegenden Daten unter Berücksichtigung des gegenwärtigen wissenschaftlichen Kontexts (Supervision durch Prof. Dr. Kay Raum und Prof. Dr. Michael Oelze)

Einleitung / Methodik / Ergebnisse:

- Literaturrecherche, Auswahl, Vergleich und Verifikation geeigneter statistischer Methoden für den in dieser Studie vorliegenden Anwendungsfall, Entscheidung zur Verwendung von QLS-Regression und ROC-Analyse
- Vollständige Implementierung der Datenauswertung in Matlab
- Berechnung der Klassifikationen für alle Proben

Diskussion:

- Interpretation und Diskussion der gewonnenen Daten mit fachlicher Unterstützung von Prof. Dr. Kay Raum und Diskussion mit den Ko-Autoren

Manuskript:

- Grafische Aufarbeitung der Ergebnisse
- Initialer Entwurf des gesamten Manuskripts und eigenständige Überarbeitung auf Basis der Begutachtungen der Ko-Autoren und im Rahmen des Review-Prozesses

Publikation 3: Männicke N, Schöne M, Liukkonen J, Fachet D, Inkinen S, Malo MK, Oelze ML, Töyräs J, Jurvelin JS, Raum K: Species-Independent Modeling of High-Frequency Ultrasound Backscatter in Hyaline Cartilage. Ultrasound in Medicine and Biology, Jun 2016.

80%

Beitrag im Einzelnen:

Maßgeblich verantwortlich für Planung und Erarbeitung der Zielsetzung der Studie, sowie Planung der Publikation

Methodik / Ergebnisse:

- Probenpräparation (gemeinsam mit Martin Schöne und Jukka Liukkonen)
- Durchführung der Ultraschallmessungen für alle Proben und Referenzmaterialien
- Erweiterung der in Publikation 1 entwickelten Signalauswertung zur Auswertung der Gelenkknorpeldünnschnitte
- Auswahl und Durchführung der statistischen Auswertung (multivariate Regression, Korrelationskoeffizienten)

Diskussion:

- Interpretation und Diskussion der gewonnenen Daten mit fachlicher Unterstützung von Prof. Dr. Kay Raum und Diskussion mit den Ko-Autoren

Manuskript:

- Grafische Aufarbeitung der Ergebnisse (Ausnahme: Fig. 1 erstellt durch Martin Schöne)
- Initialer Entwurf des gesamten Manuskripts und eigenständige Überarbeitung auf Basis der Begutachtungen der Ko-Autoren und im Rahmen des Review-Prozesses

Unterschrift, Datum und Stempel des betreuenden Hochschullehrers/der betreuenden Hochschullehrerin

_____

Unterschrift des Doktoranden/der Doktorandin

_____

Männicke, N., Schöne, M., Gottwald, M., Göbel, F., Oelze, M.L. and Raum, K., 2014. 3-D high-frequency ultrasound backscatter analysis of human articular cartilage. Ultrasound in Medicine and Biology, 40(1), pp.244-257.
https://doi.org/10.1016/j.ultrasmedbio.2013.08.015

Männicke, N., Schöne, M., Gottwald, M., Göbel, F., Oelze, M.L. and Raum, K., 2014. 3-D high-frequency ultrasound backscatter analysis of human articular cartilage. Ultrasound in Medicine and Biology, 40(1), pp.244-257.
https://doi.org/10.1016/j.ultrasmedbio.2013.08.015

Männicke, N., Schöne, M., Gottwald, M., Göbel, F., Oelze, M.L. and Raum, K., 2014. 3-D high-frequency ultrasound backscatter analysis of human articular cartilage. Ultrasound in Medicine and Biology, 40(1), pp.244-257.
https://doi.org/10.1016/j.ultrasmedbio.2013.08.015

Männicke, N., Schöne, M., Gottwald, M., Göbel, F., Oelze, M.L. and Raum, K., 2014. 3-D high-frequency ultrasound backscatter analysis of human articular cartilage. Ultrasound in Medicine and Biology, 40(1), pp.244-257.
https://doi.org/10.1016/j.ultrasmedbio.2013.08.015

Männicke, N., Schöne, M., Gottwald, M., Göbel, F., Oelze, M.L. and Raum, K., 2014. 3-D high-frequency ultrasound backscatter analysis of human articular cartilage. Ultrasound in Medicine and Biology, 40(1), pp.244-257.
https://doi.org/10.1016/j.ultrasmedbio.2013.08.015

Männicke, N., Schöne, M., Gottwald, M., Göbel, F., Oelze, M.L. and Raum, K., 2014. 3-D high-frequency ultrasound backscatter analysis of human articular cartilage. Ultrasound in Medicine and Biology, 40(1), pp.244-257.
https://doi.org/10.1016/j.ultrasmedbio.2013.08.015

Männicke, N., Schöne, M., Gottwald, M., Göbel, F., Oelze, M.L. and Raum, K., 2014. 3-D high-frequency ultrasound backscatter analysis of human articular cartilage. Ultrasound in Medicine and Biology, 40(1), pp.244-257.
https://doi.org/10.1016/j.ultrasmedbio.2013.08.015

Männicke, N., Schöne, M., Gottwald, M., Göbel, F., Oelze, M.L. and Raum, K., 2014. 3-D high-frequency ultrasound backscatter analysis of human articular cartilage. Ultrasound in Medicine and Biology, 40(1), pp.244-257.
https://doi.org/10.1016/j.ultrasmedbio.2013.08.015

Männicke, N., Schöne, M., Gottwald, M., Göbel, F., Oelze, M.L. and Raum, K., 2014. 3-D high-frequency ultrasound backscatter analysis of human articular cartilage. Ultrasound in Medicine and Biology, 40(1), pp.244-257.
https://doi.org/10.1016/j.ultrasmedbio.2013.08.015

Männicke, N., Schöne, M., Gottwald, M., Göbel, F., Oelze, M.L. and Raum, K., 2014. 3-D high-frequency ultrasound backscatter analysis of human articular cartilage. Ultrasound in Medicine and Biology, 40(1), pp.244-257.
https://doi.org/10.1016/j.ultrasmedbio.2013.08.015

Männicke, N., Schöne, M., Gottwald, M., Göbel, F., Oelze, M.L. and Raum, K., 2014. 3-D high-frequency ultrasound backscatter analysis of human articular cartilage. Ultrasound in Medicine and Biology, 40(1), pp.244-257.
https://doi.org/10.1016/j.ultrasmedbio.2013.08.015

Männicke, N., Schöne, M., Gottwald, M., Göbel, F., Oelze, M.L. and Raum, K., 2014. 3-D high-frequency ultrasound backscatter analysis of human articular cartilage. Ultrasound in Medicine and Biology, 40(1), pp.244-257.
https://doi.org/10.1016/j.ultrasmedbio.2013.08.015

Männicke, N., Schöne, M., Gottwald, M., Göbel, F., Oelze, M.L. and Raum, K., 2014. 3-D high-frequency ultrasound backscatter analysis of human articular cartilage. Ultrasound in Medicine and Biology, 40(1), pp.244-257.
https://doi.org/10.1016/j.ultrasmedbio.2013.08.015

Männicke, N., Schöne, M., Gottwald, M., Göbel, F., Oelze, M.L. and Raum, K., 2014. 3-D high-frequency ultrasound backscatter analysis of human articular cartilage. Ultrasound in Medicine and Biology, 40(1), pp.244-257.
https://doi.org/10.1016/j.ultrasmedbio.2013.08.015

Männicke, N., Schöne, M., Oelze, M. and Raum, K., 2014. Articular cartilage degeneration classification by means of high-frequency ultrasound. Osteoarthritis and cartilage, 22(10), pp.1577-1582. **https://doi.org/10.1016/j.joca.2014.06.019**

Männicke, N., Schöne, M., Oelze, M. and Raum, K., 2014. Articular cartilage degeneration classification by means of high-frequency ultrasound. Osteoarthritis and cartilage, 22(10), pp.1577-1582. **https://doi.org/10.1016/j.joca.2014.06.019**

Männicke, N., Schöne, M., Oelze, M. and Raum, K., 2014. Articular cartilage degeneration classification by means of high-frequency ultrasound. Osteoarthritis and cartilage, 22(10), pp.1577-1582. **https://doi.org/10.1016/j.joca.2014.06.019**

Männicke, N., Schöne, M., Oelze, M. and Raum, K., 2014. Articular cartilage degeneration classification by means of high-frequency ultrasound. Osteoarthritis and cartilage, 22(10), pp.1577-1582. **https://doi.org/10.1016/j.joca.2014.06.019**

Männicke, N., Schöne, M., Oelze, M. and Raum, K., 2014. Articular cartilage degeneration classification by means of high-frequency ultrasound. Osteoarthritis and cartilage, 22(10), pp.1577-1582. **https://doi.org/10.1016/j.joca.2014.06.019**

Männicke, N., Schöne, M., Oelze, M. and Raum, K., 2014. Articular cartilage degeneration classification by means of high-frequency ultrasound. Osteoarthritis and cartilage, 22(10), pp.1577-1582. **https://doi.org/10.1016/j.joca.2014.06.019**

Männicke, N., Schöne, M., Liukkonen, J., Fachet, D., Inkinen, S., Malo, M.K., Oelze, M.L., Töyräs, J., Jurvelin, J.S. and Raum, K., 2016. Species-independent modeling of high-frequency ultrasound backscatter in hyaline cartilage. Ultrasound in Medicine and Biology, 42(6), pp.1375-1384. **https://doi.org/10.1016/j.ultrasmedbio.2016.01.018**

Männicke, N., Schöne, M., Liukkonen, J., Fachet, D., Inkinen, S., Malo, M.K., Oelze, M.L., Töyräs, J., Jurvelin, J.S. and Raum, K., 2016. Species-independent modeling of high-frequency ultrasound backscatter in hyaline cartilage. Ultrasound in Medicine and Biology, 42(6), pp.1375-1384. **https://doi.org/10.1016/j.ultrasmedbio.2016.01.018**

Männicke, N., Schöne, M., Liukkonen, J., Fachet, D., Inkinen, S., Malo, M.K., Oelze, M.L., Töyräs, J., Jurvelin, J.S. and Raum, K., 2016. Species-independent modeling of high-frequency ultrasound backscatter in hyaline cartilage. Ultrasound in Medicine and Biology, 42(6), pp.1375-1384. **https://doi.org/10.1016/j.ultrasmedbio.2016.01.018**

Männicke, N., Schöne, M., Liukkonen, J., Fachet, D., Inkinen, S., Malo, M.K., Oelze, M.L., Töyräs, J., Jurvelin, J.S. and Raum, K., 2016. Species-independent modeling of high-frequency ultrasound backscatter in hyaline cartilage. Ultrasound in Medicine and Biology, 42(6), pp.1375-1384. **https://doi.org/10.1016/j.ultrasmedbio.2016.01.018**

Männicke, N., Schöne, M., Liukkonen, J., Fachet, D., Inkinen, S., Malo, M.K., Oelze, M.L., Töyräs, J., Jurvelin, J.S. and Raum, K., 2016. Species-independent modeling of high-frequency ultrasound backscatter in hyaline cartilage. Ultrasound in Medicine and Biology, 42(6), pp.1375-1384. **https://doi.org/10.1016/j.ultrasmedbio.2016.01.018**

Männicke, N., Schöne, M., Liukkonen, J., Fachet, D., Inkinen, S., Malo, M.K., Oelze, M.L., Töyräs, J., Jurvelin, J.S. and Raum, K., 2016. Species-independent modeling of high-frequency ultrasound backscatter in hyaline cartilage. Ultrasound in Medicine and Biology, 42(6), pp.1375-1384. **https://doi.org/10.1016/j.ultrasmedbio.2016.01.018**

Männicke, N., Schöne, M., Liukkonen, J., Fachet, D., Inkinen, S., Malo, M.K., Oelze, M.L., Töyräs, J., Jurvelin, J.S. and Raum, K., 2016. Species-independent modeling of high-frequency ultrasound backscatter in hyaline cartilage. Ultrasound in Medicine and Biology, 42(6), pp.1375-1384. **https://doi.org/10.1016/j.ultrasmedbio.2016.01.018**

Männicke, N., Schöne, M., Liukkonen, J., Fachet, D., Inkinen, S., Malo, M.K., Oelze, M.L., Töyräs, J., Jurvelin, J.S. and Raum, K., 2016. Species-independent modeling of high-frequency ultrasound backscatter in hyaline cartilage. Ultrasound in Medicine and Biology, 42(6), pp.1375-1384. **https://doi.org/10.1016/j.ultrasmedbio.2016.01.018**

Männicke, N., Schöne, M., Liukkonen, J., Fachet, D., Inkinen, S., Malo, M.K., Oelze, M.L., Töyräs, J., Jurvelin, J.S. and Raum, K., 2016. Species-independent modeling of high-frequency ultrasound backscatter in hyaline cartilage. Ultrasound in Medicine and Biology, 42(6), pp.1375-1384. **https://doi.org/10.1016/j.ultrasmedbio.2016.01.018**

Männicke, N., Schöne, M., Liukkonen, J., Fachet, D., Inkinen, S., Malo, M.K., Oelze, M.L., Töyräs, J., Jurvelin, J.S. and Raum, K., 2016. Species-independent modeling of high-frequency ultrasound backscatter in hyaline cartilage. Ultrasound in Medicine and Biology, 42(6), pp.1375-1384. **https://doi.org/10.1016/j.ultrasmedbio.2016.01.018**

Curriculum Vitae
Nils Stefan Männicke

Mein Lebenslauf wird aus datenschutzrechtlichen Gründen in der elektronischen Version meiner Arbeit nicht veröffentlicht.

Publikationsliste

Conferences

N. Männicke, M. Schöne, and K. Raum, "Integrated reflection coefficient correction with respect to surface inclination and axial distance," in *Proc. IEEE Int. Ultrasonics Symp*, pp. 2244–2247, Sept. 2009

N. Männicke, K. Raum, W. Richter, and E. Steck, "Monitoring of cartilage synthesis in tissue-engineered scaffolds by ultrasound biomicroscopy," in *World Congress on Medical Physics and Biomedical Engineering, September 7-12, 2009, Munich, Germany*, pp. 169–172, Springer, 2009

N. Männicke, T. Koch, S. Lakshmanan, D. Mörlein, and K. Raum, "Application of cepstral analysis for ultrasonic structural parameter characterization," 2010

N. Männicke, M. Schöne, M. Gottwald, F. Göbel, M. Oelze, and K. Raum, "High-frequency backscatter analysis of human articular cartilage," in *2013 IEEE International Ultrasonics Symposium (IUS)*, pp. 1228–1231, IEEE, 2013

Articles

N. Männicke, M. Schöne, M. Gottwald, F. Göbel, M. L. Oelze, and K. Raum, "3-d high-frequency ultrasound backscatter analysis of human articular cartilage," *Ultrasound Med Biol*, vol. 40, pp. 244–257, Jan. 2014

N. Männicke, M. Schöne, M. Oelze, and K. Raum, "Articular cartilage degeneration classification by means of high-frequency ultrasound," *Osteoarthritis and cartilage*, vol. 22, pp. 1577–1582, Oct. 2014

N. Männicke, M. Schöne, J. Liukkonen, D. Fachet, S. Inkinen, M. K. Malo, M. L. Oelze, J. Töyräs, J. S. Jurvelin, and K. Raum, "Species-independent modeling of high-frequency ultrasound backscatter in hyaline cartilage," *Ultrasound in medicine & biology*, vol. 42, pp. 1375–1384, June 2016

S. Lakshmanan, T. Koch, S. Brand, N. Männicke, M. Wicke, D. Mörlein, and K. Raum, "Prediction of the intramuscular fat content in loin muscle of pig carcasses by quantitative time-resolved ultrasound," *Meat.Sci.*, vol. 90, pp. 216–225, Jan. 2012

M. Schöne, N. Männicke, M. Gottwald, F. Göbel, and K. Raum, "3-d high frequency ultrasound improves the estimation of surface properties in degenerated cartilage," *Ultrasound Med.Biol.*, vol. 39, pp. 834–844, May 2013

B. Hesse, N. Männicke, A. Pacureanu, P. Varga, M. Langer, P. Maurer, F. Peyrin, and K. Raum, "Accessing osteocyte lacunar geometrical properties in human jaw bone on the submicron length scale using synchrotron radiation μct," *Journal of microscopy*, vol. 255, no. 3, pp. 158–168, 2014

B. Hesse, M. Langer, P. Varga, A. Pacureanu, P. Dong, S. Schrof, N. Männicke, H. Suhonen, C. Olivier, P. Maurer, G. Kazakia, K. Raum, and F. Peyrin, "Alterations of mass density and 3d osteocyte lacunar properties in bisphosphonate-related osteonecrotic human jaw bone, a synchrotron μct study," *PloS one*, vol. 9, no. 2, p. e88481, 2014

P. Varga, B. Hesse, M. Langer, S. Schrof, N. Männicke, H. Suhonen, A. Pacureanu, D. Pahr, F. Peyrin, and K. Raum, "Synchrotron x-ray phase nano-tomography-based analysis of the lacunar–canalicular network morphology and its relation to the strains experienced by osteocytes in situ as predicted by case-specific finite element analysis," *Biomechanics and modeling in mechanobiology*, vol. 14, no. 2, pp. 267–282, 2015

B. Hesse, P. Varga, M. Langer, A. Pacureanu, S. Schrof, N. Männicke, H. Suhonen, P. Maurer, P. Cloetens, F. Peyrin, *et al.*, "Canalicular network morphology is the major determinant of the spatial distribution of mass density in human bone tissue: Evidence by means of synchrotron radiation phase-contrast nano-ct," *Journal of Bone and Mineral Research*, vol. 30, no. 2, pp. 346–356, 2015

M. Schöne, N. Männicke, J. Somerson, B. Marquaß, R. Henkelmann, T. Aigner, K. Raum, and R. Schulz, "3d ultrasound biomicroscopy for assessment of cartilage repair tissue: volumetric characterisation and correlation to established classification systems.," *European cells & materials*, vol. 31, p. 119, 2016

Ausgewählte Publikationen

N. Männicke, M. Schöne, M. Gottwald, F. Göbel, M. L. Oelze, and K. Raum, "3-d high-frequency ultrasound backscatter analysis of human articular cartilage," *Ultrasound Med Biol*, vol. 40, pp. 244–257, Jan. 2014. Impact Factor Ultrasound in Medicine and Biology 2014: 2.214

N. Männicke, M. Schöne, M. Oelze, and K. Raum, "Articular cartilage degeneration classification by means of high-frequency ultrasound," *Osteoarthritis and cartilage*, vol. 22, pp. 1577–1582, Oct. 2014. Impact Factor Osteoarthritis and Cartilage 2014: 4.165

N. Männicke, M. Schöne, J. Liukkonen, D. Fachet, S. Inkinen, M. K. Malo, M. L. Oelze, J. Töyräs, J. S. Jurvelin, and K. Raum, "Species-independent modeling of high-frequency ultrasound backscatter in hyaline cartilage," *Ultrasound in medicine & biology*, vol. 42, pp. 1375–1384, June 2016. Impact Factor Ultrasound in Medicine and Biology 2015/2016: 2.298

Acknowledgements

I would like to thank my supervisor Prof. Dr. Kay Raum for his guidance and advice throughout my studies. The long, memorable meetings discussing and interpreting the contained results have been essential to this work and a prime source of motivation for me on a daily basis.

I also extend thanks and appreciation to my collaborators on the conducted studies. Prof. Dr. Michael Oelze, who patiently supported me in the interpretation of results and whose engaging conversations often generated many ideas for my work. Prof. Dr. Jukka Jurvelin and Prof. Dr. Juha Töyräs for the opportunity to conduct joint experiments and for their help in interpreting the results and bringing them into context. And to the Q-BAM research group for their encouragement, their inspiring discussions as well as the constructive atmosphere they provided over the years. Here, I would like to particularly thank Martin Schöne with whom I conducted and discussed all experiments and analyses, as well as Dr. Bernhard Hesse, Dr. Peter Varga and Dr. Susanne Schrof. I am also grateful to Anke Kadow-Romacker for the excellent technical support throughout my work.

Finally, I want to express my sincere gratitude to my closest friends and my family, especially my parents Andreas and Marlies, my sisters Anne and Lucie, my grandmother Lisbeth and to my life partner Salma. Your unconditional and unlimited support as well as your strong confidence in me and my work has been my major source for motivation and has helped me overcome any moments of doubt. Without you, this work surely would not have been possible.